Hindawi
Advances in Meteorology
Volume 2020, Article ID 7353482, 11 pages
https://doi.org/10.1155/2020/7353482

*Research Article*

# Evaluation of ERA-Interim Air Temperature Data over the Qilian Mountains of China

**Peng Zhao,[1] Lu Gao,[1,2,3,4] Jianhui Wei,[5] Miaomiao Ma,[6] Haijun Deng,[1,2,3,4] Jianyun Gao,[7] and Xingwei Chen[1,2,3,4]**

[1]*College of Geographical Science, Fujian Normal University, Fuzhou 350007, China*
[2]*Institute of Geography, Fujian Normal University, Fuzhou 350007, China*
[3]*Fujian Provincial Engineering Research Center for Monitoring and Accessing Terrestrial Disasters, Fujian Normal University, Fuzhou 350007, China*
[4]*State Key Laboratory of Subtropical Mountain Ecology, Fujian Normal University, Fuzhou 350007, China*
[5]*Institute of Meteorological and Climate Research, Karlsruhe Institute of Technology, Campus Alpine, Garmisch-Partenkirchen 82467, Germany*
[6]*China Institute of Water Resources and Hydropower Research, Beijing 100038, China*
[7]*Fujian Key Laboratory of Severe Weather, Fuzhou 350001, China*

Correspondence should be addressed to Lu Gao; l.gao@foxmail.com

Received 4 August 2019; Revised 23 January 2020; Accepted 10 February 2020; Published 10 April 2020

Academic Editor: Anthony R. Lupo



In this study, 2 m air temperature data from 24 meteorological stations in the Qilian Mountains (QLM) are examined to evaluate ERA-Interim reanalysis temperature data derived from the European Centre for Medium-Range Weather Forecasts (ECMWF) for the period of 1979–2017. ERA-Interim generally captures the monthly, seasonal, and annual variation very well. High daily correlations ranging from 0.956 to 0.996 indicate that ERA-Interim captures the daily temperature observations very well. However, an average root-mean-square error (RMSE) of ±2.7°C of all stations reveals that ERA-Interim should not be directly applied at individual sites. The biases are mainly attributed to the altitude differences between ERA-Interim grid points and stations. The positive trend (0.457°C/decade) is significant over the Qilian Mountains based on the 1979–2017 observations. ERA-Interim captures the warming trend very well with an increase rate of 0.384°C/decade. The observations and ERA-Interim both show the largest positive trends in summer with the values of 0.552°C/decade and 0.481°C/decade, respectively. We conclude that in general ERA-Interim captures the trend very well for observed 2 m air temperatures and ERA-Interim is generally reliable for climate change research over the Qilian Mountains.

## 1. Introduction

The Qilian Mountains (QLM), located in the northwest of China and sited at the intersection between Gansu Province and Qinghai Province, are mountainous regions with complex terrain and climate conditions. The altitude is more than 4000 m in most of QLM, and the total area is over $19.5 \times 10^4$ km$^2$ [1–3]. The QLM is an important ecological security barrier to northwestern China and also an important water source for the Yellow River basin [4]. The glaciers of QLM are important sources of fresh water for the local population and ecosystems. However, the ecological environment has been influenced significantly due to human activities in recent years, such as deforestation, overgrazing, and overexploitation of water resources [3, 5].

Conventionally, observation is the most common resource for climate change research. Unfortunately, surface meteorological stations are sparse in QLM, especially in the western QLM. Therefore, most of previous studies in QLM are based on limited observations or remote sensing data on

the climate and glacier changes in QLM [6–9]. Jiang et al. [10] found that the annual variations of ice and snow are significant along elevations based on MODIS data. Tian et al. [9] also found that the glaciers in QLM have melted significantly in the past 20 years, which may be caused by rising temperatures. Chen et al. [11] found that the yearly air temperature lapse rate (TLR) was weaker at >3000 m elevations and the seasonal TLRs were more divergent, which further bolsters the evidence of elevation-dependent climate change. Wu et al. [12] found that there is a significant time lag between vegetation and temperature at different altitudes in Qilian Mountains. Niu et al. [13] found that air temperature increases with altitude from the north edges of Hosi Corridor to the north slope of Qilian Mountains. Qing et al. [14] found that the lapse rate is around 0.48°C/100 m in 2012 based on the four weather stations in the Hulugou watershed in QLM, which is smaller than the lapse rates in other regions of QLM. Cao et al. [15] found that the annual and seasonal temperatures exhibited unanimously fluctuating warming trends, especially in winter during the 1960–2014 period based on 19 meteorological stations on the south slope of QLM. Jin et al. [16] found the temperature gradient increases with elevation in the nonglacierized area of the Laohugou basin of QLM.

Compared with reanalysis data, the observed records have some shortcomings, such as short time series and uneven temporal/spatial distributions. Spatial interpolation methods such as Kriging interpolation and inverse distance weights interpolation are usually used to estimate those regions without station observation data [17]. However, different interpolation methods often lead to large errors due to the limitations of the spatial interpolation itself, such as the density and uneven distribution of sites. Reanalysis data have been widely used in the past two decades because of their high resolution and long-time series [18, 19]. However, reanalysis data are sometimes unreliable due to their biases. (e.g., [17, 19]) evaluated the CFSR, ERA-Interim, MERRA, and MERRA-2 reanalysis data sets and found that the reanalysis data are inappropriate for use as supplementary data for offshore wind resources assessment. Auger et al. [20] found that reanalysis data exhibit significant differences over particular regions based on a global ensemble mean of the four third-generation climate reanalysis models in 1981–2010. Therefore, it is still a necessity to evaluate the quality and bias of reanalysis data.

There are many studies regarding the evaluation of ERA-Interim in different regions such as Canadian Prairies [21], the Tibetan Plateau [22], and Portugal [23]. For example, Gao et al. [22] and Wang et al. [24] have verified that the reanalysis data could be an alternative to observations in areas lacking data because of their resolution and long-time series. Liu et al. [25] concluded that the researchers should be careful when using ERA-Interim precipitation and temperature data in complex topography areas. Gao et al. [22] concluded that ERA-Interim is generally reliable for climate change studies over the Tibetan Plateau. Gao et al. [26] concluded that evaluation of ERA-20CM data is helpful for potential users of reanalysis data to determine local climate change impact assessments in China. Gao et al. [19] also found that the monthly bias is around −3.5°C for ERA-Interim in the Tibetan Plateau. However, knowledge of the reliability of reanalysis data in QLM is quite limited. Therefore, this analysis could provide a reference for reanalysis data application at the QLM.

This study uses temperature data obtained from 24 meteorological stations for the 1979–2017 time period to test the daily 2 m air temperature from ERA-Interim in QLM. This important evaluation would answer the question that whether ERA-Interim temperature is suitable for local climate studies, especially in complex terrains. The paper is organized as follows. A short overview of ERA-Interim data, meteorological observations, and evaluation methods are given in Section 2. The results and discussions are presented in Section 3, and finally the conclusions are given in Section 4.

## 2. Data and Methods

*2.1. ERA-Interim Data ($T_e$).* The ERA-Interim 2 m air temperature (00UTC, 06UTC, 12UTC, and 18UTC) data ($T_e$) were supplied by the European Centre for Medium Range Weather Forecasts (ECMWF). The spatial resolution is 0.25° × 0.25°, and the time step is 6 hours. The spatial range is 35.5°N-40.75°N, 93°E-104.5°E, and the period is from January 1979 to December 2017. ERA-Interim temperature data are calculated as daily mean temperature ($T$_mean), daily maximum temperature ($T$_max), and daily minimum temperature ($T$_min). Since the time of reanalysis data is UTC time, it matches the ground observations by using time difference conversion. The ERA-Interim modelled (point) height is calculated by dividing geopotential by gravity at each grid point (Table 1).

*2.2. Observations ($T_o$).* Daily air temperature ($T_o$) and elevation information for 24 meteorological stations from daily data set V3.0 were provided by the China Meteorological Data Sharing Service System of National Meteorological Information Center (http://data.cma.cn/) (Figure 1 and Table 1). The provider strictly controlled the quality of the observed data including 825 National Reference and Basic Stations (NRBS) over China from five aspects: climate limit value and allowable value checking, extreme value checking, internal consistency checking between timing value, daily average, and daily extreme value, time consistency checking, and space consistency checking. All the data are checked and corrected manually (http://data.cma.cn/data/cdcdetail/dataCode/SURF_CLI_CHN_MUL_DAY_V3.0.html, last access: 06 February 2020). Based on this data set, the Chinese homogenized historical temperature data set (CHHT, version 1.0) was released in 2009 [27, 28]. However, the CHHT was updated only to 2012 (http://data.cma.cn/data/cdcdetail/dataCode/SURF_CLI_CHN_TEM_MUT_HOMO.html, last access: 06 February 2020). At present, the daily data set V3.0 is the most authoritative and reliable observation data in China, which were widely applied for climate studies [19, 29, 30]. The selection criteria for stations were long-term consecutive measurement with no gaps exceeding two consecutive weeks.

Table 1: Meteorological station information.

| No. | Site name | Latitude (°) | Longitude (°) | Elevation (m) | $H_{ERA}$ (m) | $H_{ERA-Obs}$ (m) |
|---|---|---|---|---|---|---|
| 1 | Dun Huang | 40.13 | 94.78 | 1100 | 1508 | 408 |
| 2 | An Xi | 40.50 | 95.92 | 1182 | 1668 | 486 |
| 3 | Yu Menzhen | 40.27 | 97.18 | 1580 | 1869 | 289 |
| 4 | Jin Ta | 40.00 | 98.90 | 1270 | 1631 | 360 |
| 5 | Jiu Quan | 39.67 | 98.72 | 1470 | 1981 | 511 |
| 6 | Gao Tai | 39.38 | 99.72 | 1357 | 2225 | 868 |
| 7 | Zhang Ye | 38.92 | 100.58 | 1550 | 2074 | 524 |
| 8 | Shan Dan | 38.78 | 101.08 | 1760 | 2168 | 409 |
| 9 | Yong Chang | 38.23 | 101.97 | 1987 | 2277 | 291 |
| 10 | Wu Wei | 38.08 | 102.92 | 1525 | 1940 | 415 |
| 11 | Wu Shaoling | 37.20 | 102.87 | 3045 | 2604 | -441 |
| 12 | Jing Tai | 37.23 | 104.18 | 1620 | 1761 | 141 |
| 13 | Gao Lan | 36.55 | 103.67 | 2032 | 2146 | 114 |
| 14 | Leng Hu | 38.75 | 93.58 | 2762 | 2941 | 179 |
| 15 | Tuo Le | 38.87 | 98.37 | 3460 | 3936 | 476 |
| 16 | Ye Niugou | 38.62 | 99.35 | 3200 | 3649 | 449 |
| 17 | Qi Lian | 38.18 | 100.30 | 2800 | 3346 | 546 |
| 18 | Da Chaidan | 37.83 | 95.28 | 3000 | 3364 | 364 |
| 19 | De Lingha | 37.25 | 97.13 | 2762 | 3469 | 708 |
| 20 | Gang Cha | 37.33 | 100.17 | 3100 | 3556 | 456 |
| 21 | Men Yuan | 37.45 | 101.62 | 2800 | 3309 | 509 |
| 22 | Lin Xia | 35.62 | 103.18 | 1900 | 2579 | 679 |
| 23 | Xi Ning | 36.58 | 101.92 | 2231 | 2916 | 685 |
| 24 | Min He | 36.23 | 102.93 | 1900 | 2412 | 512 |

Note: $H_{ERA}$ is the ERA-Interim grid point height (m).

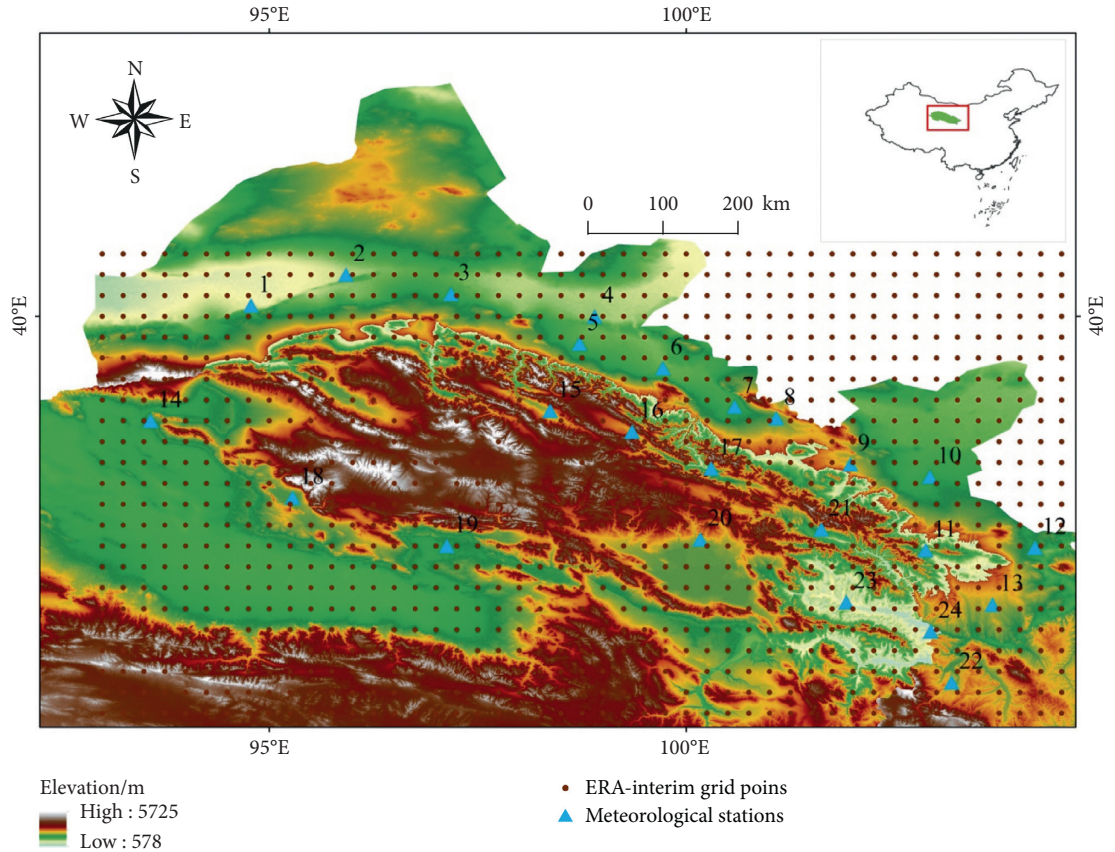


Figure 1: Locations of the 24 meteorological stations (yellow triangles) and ERA-Interim 0.25°×0.25° grid points (dots) in QLM. The numbers refer to the stations shown in Table 1.

Daily air temperature includes daily mean temperature, daily maximum temperature, and daily minimum temperature.

We have to mention that ERA-Interim latitude/longitude grids are interpolated from a reduced Gaussian grid N128 (~79 km). The grid point closest to the station is selected because the ERA-Interim grid point covers an area of $0.25^\circ \times 0.25^\circ$in which the station is located. In other words, the grid points represent the value for the whole grid. However, no matter what methods we use to interpolate ERA-Interim to individual site, it will definitely bring new errors. The traditional interpolation methods such as Kriging, Inverse Distance Weighted, and Spline have certain shortcomings in complex mountain areas [17]. Therefore, we used the variables from ERA-Interim gridded data without interpolation for a more objectively comparison. The expert (Dr. Florian Pappenberger) from the ECMWF also recommended the nearest grid point to the meteorological station in the private communication. We selected the grid point closest to the station because this ERA-Interim grid point covers the area of $0.25^\circ \times 0.25^\circ$ where the station is located. Therefore, according to the longitude and latitude coordinates of 24 meteorological stations, the corresponding grid points are selected for comparison, which can avoid the error caused by multigrid spatial interpolation [17, 31].

The 24 stations are located at different altitudes, ranging from 1000 m to 4000 m. The ERA-Interim grid point nearest to each station was extracted according to the coordinates of stations. Detailed station information is given in Figure 1 and Table 1. Elevation difference (ERA-Interim grid point height minus meteorological station height) is also listed in Table 1. In general, 23 stations have positive elevation difference, with the exception of station No. 11 having a negative elevation difference. The four seasons are defined as spring (March-May), summer (June-August), autumn (September-November), and winter (December-February).

*2.3. Evaluation Methods.* In order to evaluate the quality the ERA-Interim data set, three criteria were computed based on comparison of the ERA-Interim and observed temperatures at the 24 meteorological stations: correlation coefficient ($r$), root-mean-square-error (RMSE), and bias.

## 3. Results and Discussion

*3.1. Daily Temperature Comparisons.* The overall performance of ERA-Interim daily air temperature in 1979–2017, with respect to daily mean temperature ($T$_mean), daily maximum temperature ($T$_max), and daily minimum temperature ($T$_min), is listed in Table 2. The correlation coefficient ($r$) ranges from 0.956 to 0.996 for the three temperatures. The high $r$ indicates that $T_e$ captures the daily observations very well. The biases of daily mean temperature range from −3.9°C to +2.8°C with an average value of −1.8°C. The positive values indicate that $T_e$ is warmer than $T_o$ and the negative values reveal that $T_e$ is cooler than $T_o$. The largest positive bias (+2.8°C) is found at station No. 11 (Wu Shaoling in Gansu Province), which is located in the east of QLM. The grid height (2604 m) is much lower than the station Wu Shaoling (3045 m). The largest negative bias (−3.9°C) is found at station No. 15 (Tuo Le in Qinghai Province) situated at an elevation of 3460 meters in the northern QLM. However $T_e$ was modelled at the grid point height of 3936m. The second highest negative bias (−3.5°C) appears for station No. 6 (Gao Tai) which is at an altitude only of 1357 m, while the ERA-Interim grid height is much higher (2225 m). We selected another three typical stations: station No. 14, station No. 19, and station No. 20 as representative sites, which are distributed in the western and southern boundary of QLM. The daily biases are −1.0°C, −3.4°C, and −2.5°C for these three stations, respectively. Figure 2 shows the comparison of ERA-Interim daily reanalysis with observations of station No. 6, No. 11, No. 14, No. 15, No. 19, and No. 20 in 1979–2017. ERA-Interim underestimates significantly the temperature at station No. 15 while it overestimates at No. 11. Other stations performed very well along the 1 : 1 line. The RMSE of $T$_mean changes from ±1.4°C to ±4.5°C for all stations. The largest RMSE for $T$_mean is also found at station No. 15, while the lowest RMSE values are found at station No. 1, No. 3, and No. 4. The averaged RMSE is ±2.7°C for all stations, which suggests that $T_e$ may be questionable for direct application into climatological and hydrological studies.

For daily maximum temperature, the bias of daily maximum temperature ranges from −7.0°C to +2.9°C with an average value of −4.0°C. Positive values indicate that $T_e$ is warmer than $T_o$ and negative values show that $T_e$ is colder than $T_o$. The largest warm bias (+2.9°C) happens at station No. 11 (Wu Shaoling in Gansu Province), which is located in the east of QLM. The grid height (2604 m) is lower than the height of station Wu Shaoling (3045 m). The largest cold bias (−7.0°C) comes out at station No. 15 (Tuo Le in Qinghai Province) with an elevation of 3460 m in the northern QLM. However, $T_e$ is modelled at the grid point height of 3936 m. The RMSE ranges from ±2.9°C to ±7.4°C. Station No. 15 has the largest RMSE, while station No. 12 has the smallest one. The averaged RMSE for all stations is ±4.7°C.

For daily minimum temperature, the bias ranges from −2.6°C to +2.8°C with an average value of −0.1°C. The positive values indicate that $T_e$ is warmer than $T_o$ and the negative values mean that $T_e$ is colder than $T_o$. The largest warm bias (+2.8°C) happened at station No. 11 (Wu Shaoling) located in the east of QLM. The grid height (2604 m) is lower than the height of station Wu Shaoling (3045 m). Station No. 19 (De Lingha in Qinghai Province) has the largest cold bias (−2.6°C). Its elevation is 2762 m in the northern QLM. However, $T_e$ was modelled at 3469 m grid height. RMSE ranges from ±1.9°C to ±3.8°C. Station No. 11 has the largest RMSE while station No. 5 has the smallest one. The averaged RMSE is ±2.7°C over all stations.

*3.2. Monthly and Seasonal Mean Temperature Comparisons.* Table S1shows the monthly bias between ERA-Interim reanalysis and observations. In general, the largest positive bias is found at station No. 11 while the largest negative biases are

Table 2: Comparison of ERA-Interim daily temperature with observations at all 24 stations.

| No. | $r$ | | | Bias (°C) | | | RMSE (°C) | | |
|---|---|---|---|---|---|---|---|---|---|
| | $T$_mean | $T$_max | $T$_min | $T$_mean | $T$_max | $T$_min | $T$_mean | $T$_max | $T$_min |
| 1 | 0.994 | 0.988 | 0.986 | −0.4 | −2.8 | +1.3 | ±1.4 | ±3.5 | ±2.3 |
| 2 | 0.992 | 0.987 | 0.976 | −1.2 | −4.1 | +0.7 | ±2.1 | ±4.6 | ±2.8 |
| 3 | 0.996 | 0.990 | 0.985 | −0.7 | −2.6 | +1.2 | ±1.4 | ±3.2 | ±2.2 |
| 4 | 0.995 | 0.991 | 0.986 | −0.7 | −3.1 | +1.5 | ±1.4 | ±3.6 | ±2.4 |
| 5 | 0.994 | 0.989 | 0.985 | −1.8 | −3.6 | −0.2 | ±2.3 | ±4.1 | ±1.9 |
| 6 | 0.989 | 0.982 | 0.975 | −3.5 | −6.1 | −1.2 | ±4.0 | ±6.6 | ±2.7 |
| 7 | 0.988 | 0.982 | 0.974 | −2.3 | −5.1 | +0.1 | ±3.0 | ±5.6 | ±2.6 |
| 8 | 0.992 | 0.984 | 0.982 | −2.1 | −4.4 | −0.1 | ±2.5 | ±4.8 | ±2.0 |
| 9 | 0.990 | 0.981 | 0.977 | −1.0 | −2.7 | +0.8 | ±1.8 | ±3.3 | ±2.3 |
| 10 | 0.991 | 0.985 | 0.980 | −1.8 | −3.2 | +0.1 | ±2.3 | ±3.7 | ±2.2 |
| 11 | 0.978 | 0.973 | 0.967 | +2.8 | +2.9 | +2.8 | ±3.4 | ±3.6 | ±3.8 |
| 12 | 0.993 | 0.988 | 0.983 | −1.3 | −2.4 | −0.6 | ±1.9 | ±2.9 | ±2.4 |
| 13 | 0.987 | 0.982 | 0.972 | −1.1 | −3.7 | +1.0 | ±2.1 | ±4.3 | ±2.7 |
| 14 | 0.992 | 0.989 | 0.976 | −1.0 | −3.9 | +1.4 | ±1.8 | ±4.1 | ±2.9 |
| 15 | 0.983 | 0.977 | 0.969 | −3.9 | −7.0 | −1.0 | ±4.5 | ±7.4 | ±3.2 |
| 16 | 0.978 | 0.966 | 0.964 | −1.5 | −4.9 | +1.1 | ±2.7 | ±5.4 | ±3.3 |
| 17 | 0.986 | 0.973 | 0.975 | −3.3 | −6.5 | −1.1 | ±3.8 | ±6.9 | ±2.5 |
| 18 | 0.994 | 0.989 | 0.983 | −1.3 | −3.7 | +0.9 | ±1.7 | ±4.0 | ±2.2 |
| 19 | 0.991 | 0.987 | 0.979 | −3.4 | −5.4 | −2.6 | ±3.6 | ±5.7 | ±3.4 |
| 20 | 0.988 | 0.979 | 0.976 | −2.5 | −4.4 | −1.1 | ±2.9 | ±4.7 | ±2.4 |
| 21 | 0.976 | 0.963 | 0.956 | −2.6 | −5.2 | −0.5 | ±3.3 | ±5.7 | ±3.0 |
| 22 | 0.987 | 0.969 | 0.977 | −2.9 | −4.2 | −1.9 | ±3.3 | ±4.9 | ±2.7 |
| 23 | 0.986 | 0.972 | 0.970 | −3.2 | −5.6 | −1.9 | ±3.5 | ±6.0 | ±3.0 |
| 24 | 0.989 | 0.975 | 0.978 | −3.0 | −4.4 | −2.3 | ±3.3 | ±4.9 | ±3.0 |

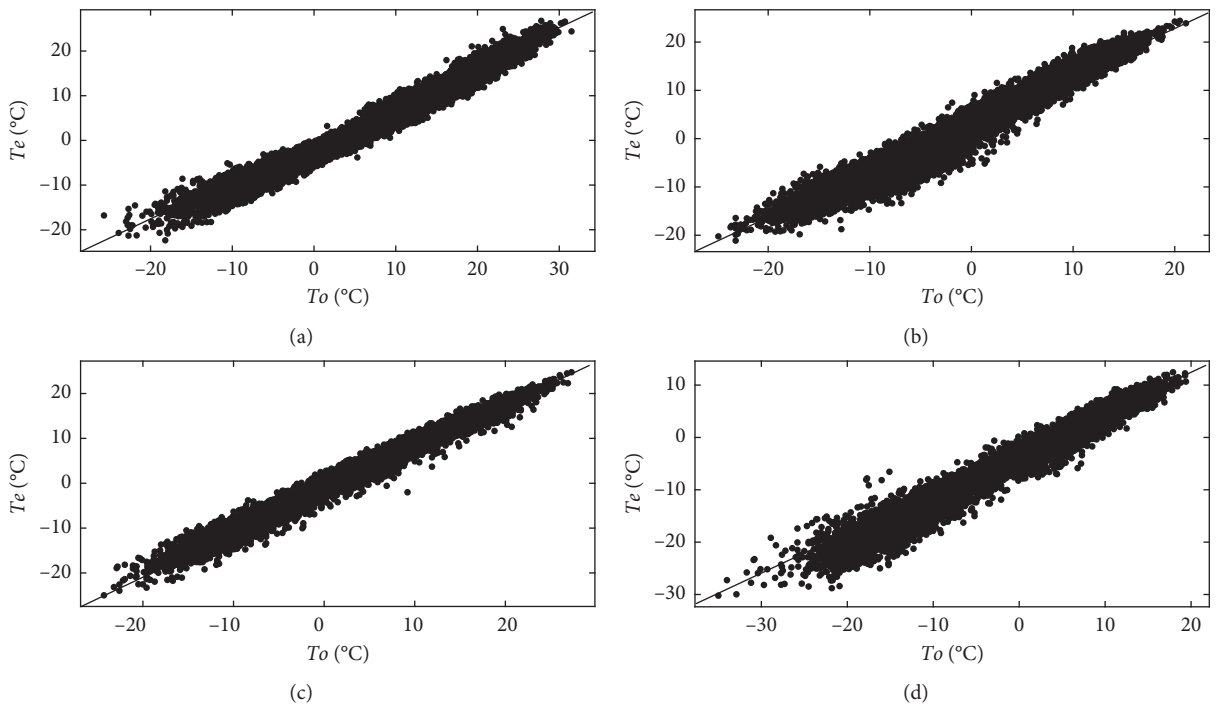


Figure 2: Continued.

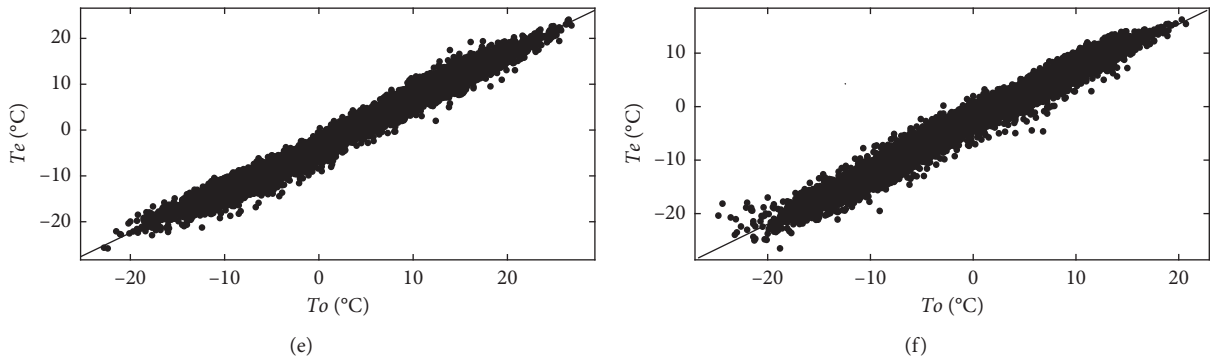


Figure 2: Scatter plots of comparison of ERA-Interim daily temperature with observations at station No. 6, No. 11, No. 14, No. 15, No. 19, and No. 20 in 1979–2017. The solid line is 1 : 1 line. (a) Station No. 6. (b) Station No. 11. (c) Station No. 14. (d) Station No. 15. (e) Station No. 19. (f) Station No. 20.

found at stations No. 6 and No. 15, which are similar with daily mean temperature. In summary, the largest negative bias at all stations is in April (-2.5°C), and the smallest negative bias at all stations is in December (-0.8°C).

The high values of $r$ mean a good agreement between $T_e$ and $T_o$ at the seasonal scale. However, the seasonal variability that reflects the year-to-year fluctuations in the seasonal means is not accordant. Table 3 shows the $r$, bias, and RMSE between $T_e$ and $T_o$. The averaged $r$ over all stations for spring, summer, autumn, and winter is 0.939, 0.910, 0.873, and 0.906, respectively. 23 stations have correlation coefficients exceeding 0.8 in spring and summer, while 22 stations meet this criterion during autumn and winter. In general, the performance of $T_e$ is really different from station to station. For example, stations No. 4 and No. 3 have the best $r$ in spring. However, for stations No. 1 and No. 18, summer has the best correlation. It shows a significant spatial variability across QLM.

The largest positive bias for all seasons is also found at station No. 11, and the greatest negative bias for all seasons is found at stations No. 6 and No. 15, which are identical with daily and monthly biases. The largest RMSE in spring is found at station No. 6 (±4.8°C). The largest RMSE in summer is found at station No. 15 (±5.7°C). The largest RMSE in autumn is found at stations No. 15 and No. 17 (±3.6°C). The largest RMSE in winter happens at station No. 19 (±3.6°C). The averaged RMSE in spring, summer, autumn, and winter is ±2.6°C, ±2.4°C, ±2.1°C, and ±1.5°C for all 24 stations, respectively.

*3.3. Annual Temperature Comparisons.* A good agreement between $T_e$ and $T_o$ at an annual scale does not imply an accordant interannual variability. Table S2 shows the correlations, bias, and RMSE of annual mean temperature between $T_e$ and $T_o$. The $r$ changes from 0.385 to 0.987 over all stations with an average of 0.892. 23 stations have better $r$ than 0.8, and only station No. 23 has a lower $r$ than 0.5. The largest positive bias (+2.8°C) is found at station No. 11. The greatest negative bias (−3.9°C) is found at station No. 15. The largest RMSE (±3.9°C) occurs at station No. 15, while the smallest RMSE (±0.4°C) is tested at station No. 1. The annual averaged RMSE over all stations is ±2.1°C.

*3.4. Warming Trends of ERA-Interim Temperature and Observations.* Figure 3 shows the aggregated annual temperatures from $T_e$ and $T_o$ as well as the temperature trends over the whole QLM. The linear increasing rate of $T_o$ is about +0.457°C/decade during the 1979–2017 period. The $T_e$ has an increasing trend of +0.384°C/decade, which means that ERA-Interim generally captures the warming trend well (Table 4). The trend difference between $T_e$ and $T_o$ is 0.076°C/decade for annual mean temperature. The largest trend difference is found in winter (0.093°C/decade). ERA-Interim captures the trends in spring, summer, and autumn very well, with values of 0.077°C/decade, 0.071°C/decade, and 0.051°C/decade, respectively. The sparse observations in the western QLM are possibly responsible for the difference. Generally, $T_e$ is reliable for the warming trend detection over QLM because $T_e$ only has an averaged 0.073°C/decade trend difference against $T_o$. However, the averaged RMSE (±2.7°C) should be given enough attention (i.e., bias correction) before $T_e$ is applied at local scale.

*3.5. Bias Analysis.* Figure 4 shows the correlation of daily biases and elevation differences between $T_e$ and $T_o$. Please note that bias and elevation difference were calculated by subtracting $T_o$ from $T_e$. The correlation of determination ($R^2$) measuring the fit is 0.762, which reveals that the altitude differences between ERA-Interim grid points and meteorological stations cause the bias. Therefore, it is possible to reduce the bias between ERA-Interim reanalysis and observations by using an elevation correction method, in order to improve the applicability of ERA-Interim [17, 26].

Spring, summer, autumn, and winter $R^2$ values are 0.837, 0.713, 0.725, and 0.381, respectively, and the annual correlation is 0.762 (Figure 5), which suggests again that altitude differences are responsible for the biases. Particularly with respect to spring temperature, the elevation difference is the main error source, indicating that elevation correction could reduce the error and further improve the applicability of ERA-Interim reanalysis. Assimilation data error, model system error, and interpolation error are also possible.

Table 5, Table 6, and Table S3 represent the averaged $r$, bias, and RMSE for different elevation groups. We divide elevation into five classifications: 1000–1500 m (5 stations),

Table 3: Comparison of ERA-Interim seasonal mean temperature with observations at all 24 stations.

| No. | $R$ | | | | Bias (°C) | | | | RMSE (°C) | | | |
|---|---|---|---|---|---|---|---|---|---|---|---|---|
| | Spring | Summer | Autumn | Winter | Spring | Summer | Autumn | Winter | Spring | Summer | Autumn | Winter |
| 1 | 0.983 | 0.981 | 0.961 | 0.970 | −1.3 | −0.5 | −0.2 | +0.4 | ±1.3 | ±0.6 | ±0.3 | ±0.5 |
| 2 | 0.988 | 0.973 | 0.942 | 0.937 | −2.2 | −1.8 | −1.0 | +0.4 | ±2.2 | ±1.8 | ±1.1 | ±0.6 |
| 3 | 0.989 | 0.957 | 0.954 | 0.982 | −1.1 | −0.9 | −0.9 | +0.3 | ±1.2 | ±0.9 | ±0.9 | ±0.4 |
| 4 | 0.991 | 0.975 | 0.958 | 0.965 | −1.3 | −0.9 | −0.7 | 0.0 | ±1.3 | ±0.9 | ±0.7 | ±0.3 |
| 5 | 0.981 | 0.951 | 0.909 | 0.972 | −2.5 | −1.9 | −1.9 | −0.9 | ±2.6 | ±1.9 | ±2.0 | ±1.0 |
| 6 | 0.956 | 0.891 | 0.857 | 0.946 | −4.7 | −4.3 | −3.4 | −1.5 | ±4.8 | ±4.3 | ±3.4 | ±1.6 |
| 7 | 0.952 | 0.904 | 0.832 | 0.934 | −3.6 | −2.8 | −2.2 | −0.6 | ±3.6 | ±2.8 | ±2.3 | ±0.8 |
| 8 | 0.969 | 0.933 | 0.917 | 0.892 | −2.5 | −2.0 | −2.3 | −1.4 | ±2.5 | ±2.0 | ±2.4 | ±1.5 |
| 9 | 0.971 | 0.904 | 0.885 | 0.941 | −1.5 | −0.6 | −1.4 | −0.5 | ±1.5 | ±0.7 | ±1.5 | ±0.6 |
| 10 | 0.963 | 0.919 | 0.818 | 0.888 | −2.3 | −1.4 | −1.9 | −1.5 | ±2.4 | ±1.5 | ±2.0 | ±1.6 |
| 11 | 0.965 | 0.872 | 0.918 | 0.943 | +3.6 | +3.9 | +2.3 | +1.5 | ±3.6 | ±3.9 | ±2.4 | ±1.6 |
| 12 | 0.961 | 0.916 | 0.876 | 0.922 | −1.5 | −0.4 | −1.4 | −2.1 | ±1.5 | ±0.5 | ±1.5 | ±2.1 |
| 13 | 0.960 | 0.942 | 0.900 | 0.924 | −2.0 | −1.3 | −1.2 | +0.3 | ±2.0 | ±1.4 | ±1.3 | ±0.5 |
| 14 | 0.922 | 0.955 | 0.936 | 0.934 | −0.9 | −1.8 | −0.9 | −0.7 | ±0.9 | ±1.8 | ±0.9 | ±0.8 |
| 15 | 0.932 | 0.955 | 0.833 | 0.891 | −4.1 | −5.7 | −3.6 | −2.1 | ±4.1 | ±5.7 | ±3.6 | ±2.1 |
| 16 | 0.881 | 0.928 | 0.742 | 0.830 | −1.7 | −2.6 | −1.4 | −0.3 | ±1.7 | ±2.6 | ±1.6 | ±0.6 |
| 17 | 0.896 | 0.891 | 0.846 | 0.921 | −3.8 | −3.9 | −3.5 | −2.1 | ±3.8 | ±3.9 | ±3.5 | ±2.2 |
| 18 | 0.958 | 0.976 | 0.951 | 0.901 | −1.2 | −1.4 | −1.2 | −1.3 | ±1.2 | ±1.4 | ±1.2 | ±1.4 |
| 19 | 0.951 | 0.942 | 0.938 | 0.929 | −3.7 | −3.0 | −3.2 | −3.6 | ±3.7 | ±3.0 | ±3.2 | ±3.6 |
| 20 | 0.930 | 0.847 | 0.876 | 0.890 | −2.4 | −2.6 | −2.2 | −2.9 | ±2.4 | ±2.7 | ±2.2 | ±3.0 |
| 21 | 0.902 | 0.805 | 0.826 | 0.721 | −3.1 | −2.7 | −2.6 | −1.9 | ±3.1 | ±2.8 | ±2.6 | ±2.1 |
| 22 | 0.891 | 0.842 | 0.902 | 0.932 | −3.8 | −3.3 | −3.1 | −1.5 | ±3.8 | ±3.4 | ±3.1 | ±1.6 |
| 23 | 0.702 | 0.708 | 0.489 | 0.630 | −3.9 | −3.1 | −3.2 | −2.4 | ±3.9 | ±3.2 | ±3.3 | ±2.6 |
| 24 | 0.931 | 0.866 | 0.891 | 0.960 | −3.8 | −3.0 | −3.2 | −2.0 | ±3.8 | ±3.0 | ±3.2 | ±2.1 |

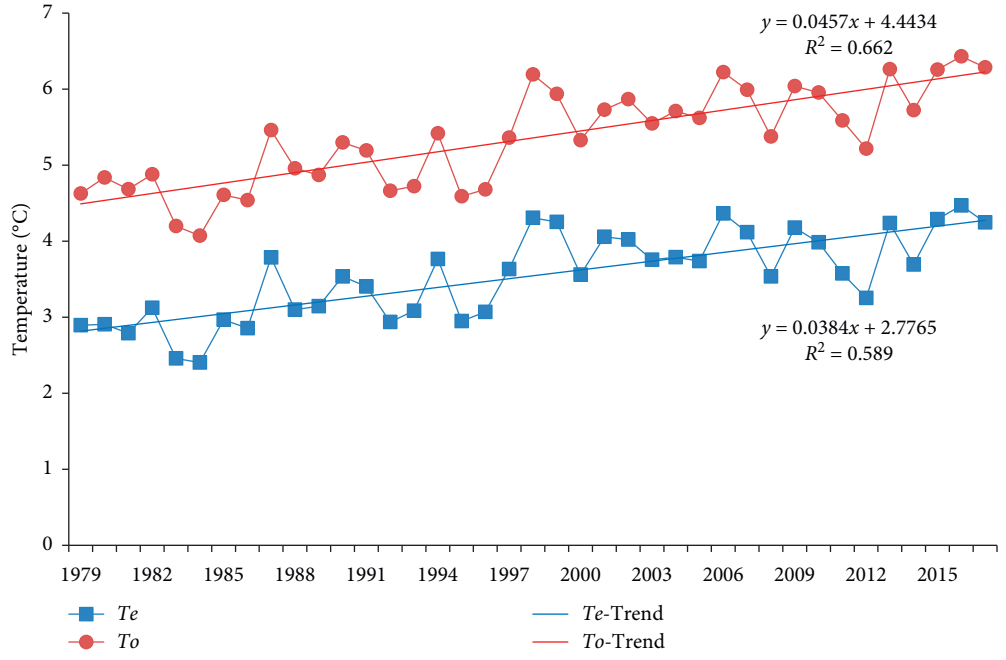


Figure 3: Average annual and seasonal mean temperature from station time series and ERA-Interim in the 1979–2017 period for QLM. The temperature trends are also shown for the two data sets.

Table 4: Temperature warming trends (°C/decade) in all seasons from station time series and ERA-Interim reanalysis in 1979–2017.

| Temperature | Spring | Summer | Autumn | Winter | Annual |
|---|---|---|---|---|---|
| $T_o$ | +0.536 | +0.552 | +0.402 | +0.336 | +0.457 |
| $T_e$ | +0.459 | +0.481 | +0.351 | +0.243 | +0.384 |
| $T_o - T_e$ | 0.077 | 0.071 | 0.051 | 0.093 | 0.073 |

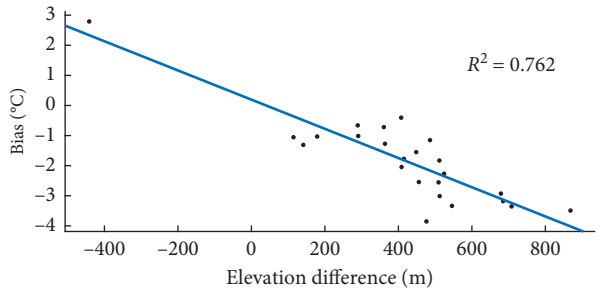


Figure 4: Relationship of bias and elevation differences between daily observations and ERA-Interim during the 1979–2017 period.

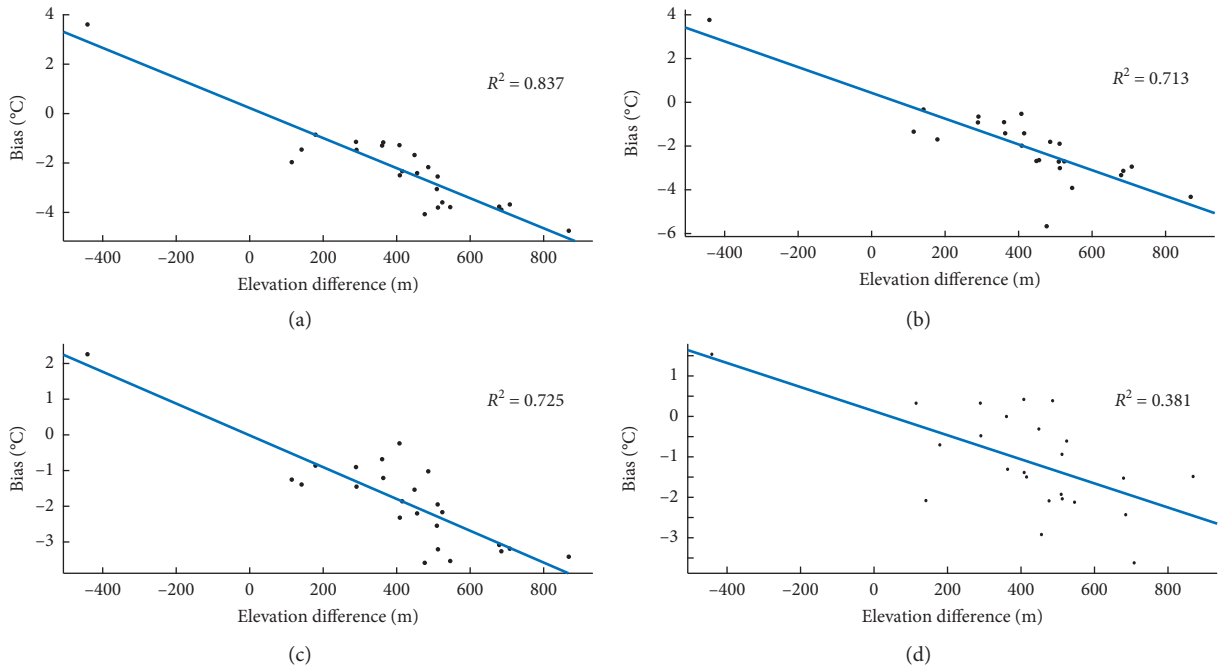


Figure 5: Relationship of bias and elevation differences between observations and ERA-Interim reanalysis in seasonal scales. (a) Spring. (b) Summer. (c) Autumn. (d) Winter.

Table 5: Daily averaged ($r$), bias, and RMSE for different elevation groups.

| $t$ | $r$ | | | Bias (°C) | | | RMSE (°C) | | |
|---|---|---|---|---|---|---|---|---|---|
| | $T$_mean | $T$_max | $T$_min | $T$_mean | $T$_max | $T$_min | $T$_mean | $T$_max | $T$_min |
| 1000–1500 | 0.994 | 0.989 | 0.984 | −1.5 | −3.9 | +0.4 | ±2.3 | ±4.5 | ±2.5 |
| 1500–2000 | 0.989 | 0.983 | 0.977 | −1.9 | −3.6 | −0.3 | ±2.4 | ±4.2 | ±2.4 |
| 2000–2500 | 0.988 | 0.983 | 0.973 | −2.1 | −4.7 | −0.5 | ±2.8 | ±5.1 | ±2.8 |
| 2500–3000 | 0.989 | 0.980 | 0.976 | −2.3 | −5.0 | −0.4 | ±2.8 | ±5.3 | ±2.8 |
| 3000–3500 | 0.984 | 0.970 | 0.970 | −1.3 | −3.4 | +0.4 | ±3.4 | ±5.3 | ±3.2 |

Table 6: Seasonal averaged ($r$), bias, and RMSE for different elevation groups.

| | $R$ | | | | Bias (°C) | | | | RMSE (°C) | | | |
|---|---|---|---|---|---|---|---|---|---|---|---|---|
| | Spring | Summer | Autumn | Winter | Spring | Summer | Autumn | Winter | Spring | Summer | Autumn | Winter |
| 1000–1500 | 0.980 | 0.954 | 0.925 | 0.958 | −2.4 | −1.9 | −1.5 | −0.3 | ±2.4 | ±1.9 | ±1.5 | ±0.8 |
| 1500–2000 | 0.953 | 0.905 | 0.884 | 0.931 | −2.5 | −1.8 | −2.0 | −1.2 | ±2.5 | ±1.9 | ±2.1 | ±1.3 |
| 2000–2500 | 0.831 | 0.825 | 0.695 | 0.777 | −2.9 | −2.2 | −2.3 | −1.1 | ±3.0 | ±2.3 | ±2.3 | ±1.5 |
| 2500–3000 | 0.926 | 0.914 | 0.899 | 0.881 | −2.5 | −2.5 | −2.3 | −1.9 | ±2.5 | ±2.6 | ±2.3 | ±2.0 |
| 3000–3500 | 0.927 | 0.901 | 0.842 | 0.889 | −1.1 | −1.8 | −1.3 | −0.9 | ±3.0 | ±3.8 | ±2.5 | ±1.8 |

1500–2000 m (8 stations), 2000–2500 m (2 stations), 2500–3000 m (5 stations), and 3000–3500 m (4 stations). In general, averaged $r$ ranges from 0.970 to 0.994 for the three temperatures for different elevation groups. Daily averaged biases are distinguished for different elevation groups. The largest negative bias (−2.3°C) of $T$_mean is found for the 2500–3000 m group, and the smallest negative bias (−1.3°C) of $T$_mean is found for the 3000–3500 m group. The largest negative bias (−5.0°C) of $T$_max is found for the 2500–3000 m group, and the smallest negative bias (−3.4°C) of $T$_max is found for the 3000–3500 m group. The largest negative bias (−0.5°C) of $T$_min is found for the 2000–2500 m group, and the largest positive bias (+0.4°C) of $T$_min is found for the 3000–3500 m group. In general, RMSE increases with the rise of elevation group. The largest RMSEs of $T$_mean and $T$_min are found for the 3000–3500 m group, and largest RMSE of $T$_max is found for the 2500–3000 m group.

Seasonal averaged $r$, bias, and RMSE are distinguished among different elevation groups. Averaged $r$ ranges from 0.695 to 0.980 for four seasons for different elevation groups. The largest negative bias (−2.9°C) in spring is found in the 2000–2500 m elevation group, and the smallest negative bias (−1.1°C) is found in the 3000–3500 m group. The largest negative bias (−2.5°C) in summer is found in the 2500–3000 m group, and the smallest negative bias (−1.8°C) is found in the 3000–3500 m group. The largest negative bias (−2.3°C) in autumn is found in the 2500–3000 m group, and the smallest negative bias (−1.2°C) is found in the 3000–3500 m group. The largest negative bias (−1.9°C) in winter is found in the 2500–3000 m elevation group, and the smallest negative bias (−0.3°C) is found in the 1000–1500 m group. In general, seasonal averaged RMSE shows an increasing trend with rising altitude. Annual averaged $r$ ranges from 0.672 to 0.959. The largest negative bias (−2.3°C) is found in the 2500–3000 m elevation group, and the smallest negative bias (−1.3°C) is found in the 3000–3500 m group.

## 4. Conclusions

In this study, ERA-Interim temperatures ($T_e$) are compared with observations ($T_o$) from 24 meteorological stations over the Qilian Mountains of China (QLM) at multiple temporal scales. High daily correlations from 0.956 to 0.996 indicate that ERA-Interim could capture the cycle very well. The biases of daily mean temperature ranging from −3.9°C to +2.8°C (averaged −1.8°C) are mainly from altitude differences between ERA-Interim grid height and the elevation of observing stations ($R^2 = 0.762$). The biases of daily maximum temperature range from −7.0°C to +2.9°C with an average value of −4.0°C. The biases of daily minimum temperature range from −2.6°C to +2.8°C with an average value of −0.1°C. The average RMSEs of daily mean temperature, daily maximum temperature, and daily minimum temperature are ±2.7°C, ±4.7°C, and ±2.7°C, respectively. The results of this comparison indicate that ERA-Interim reanalysis should not be applied directly at the local scale for climatological and hydrological model purposes due to large biases.

Monthly biases are similar to daily biases. For monthly bias variability, the largest negative bias is in April (−2.5°C), and the smallest negative bias is in December (−0.8°C). The average correlations for spring, summer, autumn, and winter are 0.939, 0.910, 0.873, and 0.906, respectively, which suggest that that ERA-Interim can reproduce the interannual variability over the QLM. Spring, summer, autumn, and winter RMSE values' biases are ±2.6°C, ±2.4°C, ±2.1°C, and ±1.5°C, respectively, which also indicate that $T_e$ could not be used directly in scientific studies. The biases in temperatures are mainly due to altitude differences, especially during the spring months ($R^2 = 0.837$). This suggests that elevation correction could reduce the error and further improve the applicability of ERA-Interim reanalysis. The relationship ($R^2$) of bias and elevation differences between seasonal observations and ERA-Interim reanalysis are 0.713, 0.725, and 0.381, for summer, autumn, and winter, respectively. The winter climate in mountain areas is more complex and changeable due to impact factors such as "cold lake." Thus, the correlation between temperature and elevation is relatively weak. For annual variability, an average correlation is 0.906 for all stations. The average annual RMSE is ±2.1°C, which also indicates that $T_e$ could not be used directly in scientific studies.

A significant warming trend (+0.457°C/decade) is detected over QLM based on observations over the 1979–2017 period. ERA-Interim can generally reproduce the warming trend at the rate of +0.384°C/decade. The largest warming trends are both detected in summer for the observations and ERA-Interim, +0.552°C/decade and +0.481°C/decade, respectively. The seasonal warming trend differences between observation and ERA-Interim are lower than 0.1°C/decade. Generally, ERA-Interim is reliable for warming trend detection over the QLM.

ERA-Interim has different performances at different altitudes. Generally, RMSE increases along higher elevations. The largest RMSE for daily $T$_mean and $T$_min is found in the 3000–3500 m elevation group, and for $T$_max it is found in the 2500–3000 m group. It indicated that ERA-Interim may be weaker for the regions that are higher than the ERA-Interim model height.

By now, this evaluation is limited to 24 meteorological stations' range in elevation from 1000 m to 4000 m. The analysis can be further extended by adding more observations in the surrounding areas. It should also be worth trying to investigate other meteorological elements of ERA-Interim reanalysis such as precipitation and humidity over the QLM.

## Data Availability

The ERA-Interim data used in this paper are provided by the European Centre for Medium-Range Weather Forecasts (ECMWF). Station data are provided at China Meteorological Data Sharing Service System of National Meteorological Information Centre (http://data.cma.cn/, last access: 06 February 2020).

## Conflicts of Interest

The authors declare that there are no conflicts of interest in this paper.

## Acknowledgments

This study was supported by the National Key Program for Developing Basic Science (Grant nos. 2018YFC1505805 and 2018YFC1508803), the Research and Development Support Program of the China Institute of Water Resources and Hydropower Research (IWHR) (Grant no. JZ0145B582017), and the Outstanding Young Scientific Research Talents Cultivation Program, Education Department of Fujian Province. Dr. Jianhui Wei was supported financially by the German Research Foundation through funding of the AccHydro project (DFG-Grant KU 2090/11-1). ERA-Interim data were supported by the ECMWF (https://www.ecmwf.int/en/forecasts/datasets). The meteorological data have been provided by China Meteorological Data Sharing Service System of National Meteorological Information Center (CMA-CMDC, http://data.cma.cn/).

## Supplementary Materials

Table S1: bias of monthly mean temperature (℃) between ERA-Interim and observations at all 24 stations in 1979–2017. Table S2: comparison of ERA-Interim annual mean temperature with observations at all 24 stations in 1979–2017. Table S3: annual averaged *r*, bias, and RMSE for different elevation groups in 1979–2017. (*Supplementary Materials*)

## References

[1] S. Zhao, W. Cheng, C. Zhou, X. au, and J. Chen, "Simulation of decadal alpine permafrost distributions in the Qilian Mountains over past 50years by using Logistic Regression Model," *Cold Regions Science and Technology*, vol. 73, no. 1, pp. 32–40, 2012.

[2] W. Sun, X. Qin, J. Ren et al., "The surface energy budget in the accumulation zone of the Laohugou glacier No. 12 in the Western Qilian Mountains, China, in summer 2009," *Arctic, Antarctic, and Alpine Research*, vol. 44, no. 3, pp. 296–305, 2012.

[3] W. Yang, Y. Wang, S. Wang et al., "Spatial distribution of Qinghai spruce forests and the thresholds of influencing factors in a small catchment, Qilian Mountains, Northwest China," *Scientific Reports*, vol. 7, no. 1, pp. 1–12, 2017.

[4] W. Wang, X. Liu, X. Shao et al., "Differential response of Qilian juniper radial growth to climate varintions in the middle of Qilian Mountains and the northeastern Qaidam Basin," *Climatic Change*, vol. 2015, no. 133, pp. 237–251, 2015.

[5] M. Yan, X. Tian, Z. Li, E. au, C. Chen, and W. Fan, "A long-term simulation of forest carbon fluxes over the Qilian Mountains," *International Journal of Applied Earth Observation and Geoinformation*, vol. 52, no. 52, pp. 515–526, 2016.

[6] J. He, W. Zhang, and Y. Wu, "The impact of mountain range geographic orientation on the altitude effect of precipitation δ18O in the upper reaches of the Heihe River Basin in the Qilian Mountains," *Water*, vol. 10, no. 12, pp. 1797–1812, 2018.

[7] Z. Rong, C. Y. Zhao, J. J. Liu et al., "Modeling the effect of climate change on the potential distribution of Qinghai Spruce (Picea crassifolia kom.) in Qilian Mountains," *Forests*, vol. 10, no. 62, pp. 1–15, 2019.

[8] S. Zhao, S. Zhang, W. Cheng et al., "Model simulation and prediction of Decadal Mountain permafrost distribution based on remote sensing data in the Qilian Mountains from the 1990s to the 2040s," *Remote Sensing*, vol. 11, no. 1, pp. 1–19, 2019.

[9] H. Tian, T. Yang, and Q. Liu, "Climate change and glacier area shrinkage in the Qilian mountains, China, from 1965-2010," *Annuals of Glaciology*, vol. 55, no. 56, pp. 187–197, 2014.

[10] Y. Jiang, J. Ming, P. Ma, P. au, and Z. Wang, "Variation in the snow cover on the Qilian Mountains and its causes in the early 21st century," *Geomatics, Natural Hazards and Risk*, vol. 7, no. 6, pp. 1824–1834, 2016.

[11] R. S. Chen, Y. X. Song, E. S. Kang et al., "A cryosphere-hydrology observation system in a small alpine watershed in the Qilian Mountains of China and its meteorological gradient," *Arctic, Antarctic, and Alpine Research*, vol. 46, no. 2, pp. 505–523, 2014.

[12] Z. L. Wu, W. X. Jia, Z. Zhao et al., "Spatial-temporal variations of vegetation and its correlation with climatic factors in Qilian Mountains from 2000 to 2012," *Arid Land Geography*, vol. 38, no. 6, pp. 1241–1252, 2015, in Chinese.

[13] Y. Niu, X. D. Liu, X. H. Yang et al., "The variance contrastive analysis of precipitation and air temperature change from north slope of Qilian Mountains to slope front corridor," *Journal of Central South University of Forestry & Technology*, vol. 36, no. 9, pp. 89–95, 2016, in Chinese.

[14] W. W. Qing, C. T. Han, and J. F. Liu, "A study on temperature lapse rate in Hulugou watershed, Qilian Mountains," *Journal of Lanzhou University (Natural Science)*, vol. 54, no. 1, pp. 44–50, 2018, in Chinese.

[15] G. C. Cao, J. X. Fu, L. Q. Li et al., "Analysis on temperature and spatial variations characteristic of air temperature in the south slope of Qilian Mountains and its nearby regions during the period from 1960 to 2014," *Research of Soil and Water Conservation*, vol. 25, no. 3, pp. 88–96, 2018, in Chinese.

[16] Z. Z. Jin, X. Qin, W. J. Sun et al., "Monthly variations of temperature gradient in glacierized and non-glacierized areas of the western Qilian Mountains," *Journal of Glaciology and Geography*, vol. 41, no. 2, pp. 282–292, 2019, in Chinese.

[17] L. Gao, J. Wei, L. Wang, M. au, K. Bernhardt, and X. Chen, "A high-resolution air temperature data set for the Chinese Tian Shan in 1979–2016," *Earth System Science Data*, vol. 10, no. 4, pp. 2097–2114, 2018.

[18] A. Omid, P. Adibi, and P. Irannejad, "Impact of the El Niño–Southern Oscillation on the climate of Iran using ERA-Interim data," *Climate Dynamics*, vol. 51, no. 7, pp. 2897–2911, 2018.

[19] L. Gao, M. Bernhardt, K. Schulz, X. au, Y. Chen, and M. Liu, "A first evaluation of ERA-20CM over China," *Monthly Weather Review*, vol. 144, no. 1, pp. 45–57, 2016.

[20] J. D. Auger, S. D. Birkel, K. Maasch et al., "An ensemble mean and evaluation of third generation global climate reanalysis models," *Atmosphere*, vol. 9, no. 2, pp. 1–12, 2018.

[21] A. K. Betts and A. C. M. Beljaars, "Analysis of near-surface biases in ERA-Interim over the Canadian Prairies," *Journal of Advances in Modeling Earth Systems*, vol. 5, no. 1, pp. 2158–2173, 2017.

[22] L. Gao, L. Hao, and X.-w. Chen, "Evaluation of ERA-interim monthly temperature data over the Tibetan Plateau," *Journal of Mountain Science*, vol. 11, no. 5, pp. 1154–1168, 2014.

[23] P. Paredes, D. S. Martins, L. S. Pereira, J. au, and C. Cadima, "Accuracy of daily estimation of grass reference evapotranspiration using ERA-Interim reanalysis products with

assessment of alternative bias correction schemes," *Agricultural Water Management*, vol. 210, no. 1, pp. 340–353, 2018.

[24] S. Wang, M. Zhang, M. Sun et al., "Comparison of surface air temperature derived from NCEP/DOE R2, ERA-Interim, and observations in the arid northwestern China: a consideration of altitude errors," *Theoretical and Applied Climatology*, vol. 119, no. 1-2, pp. 99–111, 2014.

[25] Z. Liu, Y. Liu, and S. Wang, "Evaluation of spatial and temporal performances of ERA-Interim precipitation and temperature in mainland China," *Journal of Climate*, vol. 11, no. 1, pp. 4347–4365, 2018.

[26] L. Gao, M. Bernhardt, and K. Schulz, "Elevation correction of ERA-Interim temperature data in the Tibetan Plateau," *International Journal of Climatology*, vol. 37, no. 9, pp. 3540–3552, 2017.

[27] W. Chen, Q. Li, X. L. Wang, S. au, L. Yang, and Y. Feng, "Homogenization of Chinese daily surface air temperatures and analysis of trends in the extreme temperature indices," *Journal of Geophysical Research: Atmospheres*, vol. 118, no. 17, pp. 9708–9720, 2013.

[28] Z. Li and Z. W. Yan, "Homogenized daily mean/maximum/minimum temperature series for China from 1960-2008," *Atmospheric and Oceanic Science Letters*, vol. 2, no. 4, pp. 237–243, 2009.

[29] B. Xiao, Y. Ma, T. Zhao et al., "Long-term trends in extreme temperature over China mainland based on homogenized dataset," *Meteorological Monthly*, vol. 42, no. 3, pp. 339–346, 2016, in Chinese.

[30] D. Wang, Q. You, Z. Jiang et al., "Analysis of extreme temperature changes in China based on the homogeneity-adjusted data," *Plateau Meteorology*, vol. 35, no. 5, pp. 1352–1363, 2016, in Chinese.

[31] L. Gao, M. Bernhardt, and K. Schulz, "Elevation correction of ERA-Interim temperature data in complex terrain," *Hydrology and Earth System Sciences*, vol. 16, no. 12, pp. 4661–4673, 2012.